

See discussions, stats, and author profiles for this publication at: <https://www.researchgate.net/publication/224203700>

# Maximum likelihood detection for single carrier — FDMA: Performance analysis

Conference Paper · December 2010

DOI: 10.1109/EEEL.2010.5662215 · Source: IEEE Xplore

CITATIONS

2

READS

144

4 authors, including:



**Mark Geles**

2 PUBLICATIONS 15 CITATIONS

[SEE PROFILE](#)



**Ofer Amrani**

Tel Aviv University

95 PUBLICATIONS 404 CITATIONS

[SEE PROFILE](#)



**A. Averbuch**

Tel Aviv University

355 PUBLICATIONS 5,240 CITATIONS

[SEE PROFILE](#)

Some of the authors of this publication are also working on these related projects:



Metal lines of micro-electronic devies [View project](#)



MultiView [View project](#)

# Maximum Likelihood Detection for Single Carrier - FDMA: Performance Analysis

M. Geles<sup>1</sup>, A. Averbuch<sup>2</sup>, O. Amrani<sup>1</sup>, D. Ezri<sup>3</sup>

<sup>1</sup>School of Electrical Engineering, Department of Systems Electrical Engineering  
Tel Aviv University, Tel Aviv 69978, Israel

<sup>2</sup>School of Computer Science  
Tel Aviv University, Tel Aviv 69978, Israel

<sup>3</sup>Greenair Wireless  
47 Herut St., Ramat Gan, Israel

November 22, 2009

## **Abstract**

Upper and lower bounds on the BER performance of the maximum likelihood detection of uncoded transmission in a SC-FDMA setting are derived for a Rayleigh fading channel. Approximated closed-form expressions are derived for the lower bound of the BER performance for high and low SNR regimes. These derivations are validated by simulation.

## **1 Introduction**

Orthogonal Frequency Division Multiplexing (OFDM) technology appears in some of the 4G standards. Its most important advantages are the ability to cope with multi-path environment and to provide flexible resource allocation. Along with its advantages, OFDM has

its own drawbacks as well. OFDM signal has high Peak to Average Power Ratio (PAPR). PAPR is a power characteristic of a radio signal. Formally, it is defined over a period of time  $[0, T]$  as

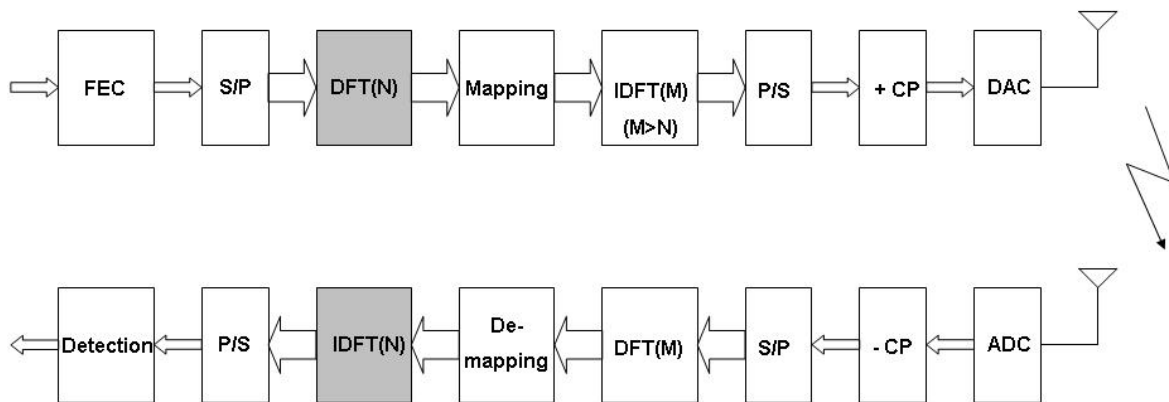
$$\text{PAPR}(x(t)) \triangleq \frac{\max_{0 < t < T} |x(t)|^2}{\frac{1}{T} \int_0^T |x(t)|^2 dt}.$$

In general, the PAPR of any transmitted signal should be as low as possible, especially at the user's equipment (UE) side. This is due to the limitation of the dynamic range of the transmitter's power amplifier. All the peaks of the transmitted signal, which exceed the dynamic range of the power amplifier, are truncated. Therefore, as the PAPR grows more of the transmitted signal is distorted by the amplifier.

The Single Carrier FDMA (SC-FDMA) provides a solution for the high OFDM PAPR issue. As in OFDM, the transmitters in a SC-FDMA system use different orthogonal frequencies (sub-carriers) to transmit information symbols. However, they transmit the sub-carriers sequentially, rather than in parallel as depicted in Fig. 1.1. Relative to OFDM, this arrangement reduces considerably the envelope fluctuations in the transmitted waveform. Therefore, SC-FDMA signals have inherently lower PAPR than OFDM signals.

There are two main SC-FDMA types: Localized SC-FDMA and distributed SC-FDMA. The distributed SC-FDMA is sometimes refereed also as interleaved SC-FDMA. In terms of PAPR reduction, the distributed SC-FDMA is superior over the localized SC-FDMA [4]. In localized SC-FDMA, the sub-carriers, which were allocated to DFT blocks, are adjacent in frequency. Therefore, for DFT sizes, which are smaller than the coherence bandwidth, the channel may be regarded as flat fading. In a distributed SC-FDMA, the sub-carriers of the user are distributed over the entire bandwidth and are equally spaced with zeros occupying the unused sub-carriers. Therefore, in a distributed SC-FDMA, channel fading is less correlated over the sub-carriers of the DFT. For example, the coherent bandwidth of the standard ITU vehicular fading channel model is about 17 sub-carriers assuming 15KHz carrier spacing. This means that a fading channel, which is experienced by a typical distributed SC-FDMA transmission, may be frequency selective. It also means that the SC-FDMA signals may arrive at a base station with substantial inter-symbol interference and the detection becomes more complicated in comparison to OFDM.

Summarizing the comparison above, by utilizing distributed SC-FDMA instead of the



S/P : serial to parallel,

P/S : parallel to serial,

DFT(x): DFT of size x,

+/- CP: addition/removal of cyclic prefix,

DAC: digital to analog converter,

ADC: analog to digital converter.




OFDMA:   
 SC-FDMA:  + 

Figure 1.1: Typical Scheme of SC-FDMA

localized SC-FDMA in a system one can achieve greater PAPR reduction [4] for the price of more complex detection at the receiver side.

Although the distributed SC-FDMA results in greater PAPR reduction, the main focus of modern technology in SC-FDMA is on the localized version of SC-FDMA. The reason is that the detection of the later is simpler. The localized version of SC-FDMA was adopted as a transmission technique by LTE ([1]), which is the next generation cellular communication standard, to handle the Uplink. A detailed introduction to SC-FDMA is given in [5].

A practical SC-FDMA detector usually involves a frequency domain equalizer (FDE). It can be Zero Forcing (ZF), MMSE, or some other linear detectors. However, for the distributed SC-FDMA (or localized SC-FDMA in severe multi-path environment), linear detectors are suboptimal. One would like to be able to compare the performance of linear detectors with the optimal Maximum Likelihood Detector (MLD). Simulating MLD is of exponential complexity and hence it cannot be performed for sufficiently large DFT size. Therefore, we want to derive an analytical expression to evaluate the MLD performance.

There are several known state-of-the-art results that analyze the performance of various detection schemes applied to a SC-FDMA transmission with different channel models. Performance analysis of ZF and MMSE linear detectors, which were applied to SC-FDMA system, is given in [6]. In addition to the exact ZF and MMSE Bit Error Rate (BER) formulae, the upper bound for MLD Packet Error Rate (PER) is given in a paper by Nisar et.al. [8]. Here, a packet means a group of modulated symbols allocated to the DFT block of the user. Thus, a packet error can be in any number of the packet bits. Therefore, BER derivation from PER is not trivial and it does not appear in [8]. In both papers ([6, 8]), the expressions are functions of the fading channel realization and they are not functions of a fading channel model.

In this work, we present lower bounds for bit error rates of MLD, which is applied to SC-FDMA setting for a particular case when the transmission is uncoded and the fading channel obeys the Rayleigh channel model. The bounds are calculated by integrating the selected error-vector probabilities w.r.t. the fading channel distribution function. The closed form expressions derived herein depend only on the size of the DFT. Furthermore Their comparison to actual simulation results are given in Section 4.

## 2 The Detection System

In this section, we describe the Maximum Likelihood Detector for SC-FDMA, which is the focus of this work. SC-FDMA differs from the regular OFDM by the application of a DFT prior to the allocation of the modulated data symbols to the OFDM sub-carriers. We concentrate on SISO SC-FDMA. The received signal in SC-FDMA time domain for a single user is

$$\mathbf{r} = \mathbf{T}\mathbf{Q}\mathbf{A}\mathbf{F}\mathbf{s} + \rho\mathbf{z}, \quad (2.1)$$

where  $\mathbf{r}$  is the received signal in time domain, the  $\mathbf{T}$  rows are cyclic shifts of the channel impulse response vector  $\mathbf{t}$ ,  $\mathbf{Q}$  is the IFFT matrix,  $\mathbf{A}$  is the allocation matrix which allocates the user's signal to its sub-carriers,  $\mathbf{F}$  is the SC DFT matrix,  $\mathbf{s}$  is a vector of  $N$  symbols ( $N$  is the DFT size) of a given modulation transmitted over  $N$  sub-carriers and  $\mathbf{z}$  is a normalized complex Gaussian noise vector. The multiplication of the vector  $\mathbf{Q}\mathbf{A}\mathbf{F}\mathbf{s}$  by the matrix  $\mathbf{T}$  represents the convolution between  $\mathbf{Q}\mathbf{A}\mathbf{F}\mathbf{s}$  and the channel response vector  $\mathbf{t}$ . Due to the fact that convolution in the time domain is equivalent to multiplication in frequency domain, we can rewrite Eq. 2.1 in the frequency domain for sufficiently long guard interval ( $>$ delay spread) as

$$\mathbf{y} = \mathbf{H}\mathbf{F}\mathbf{s} + \rho\mathbf{w}, \quad (2.2)$$

where  $\mathbf{y}$  is the received signal in the frequency domain,  $\rho\mathbf{w}$  is an additive white Gaussian noise with zero mean and standard deviation  $\rho$ . For  $i, j = 0, \dots, N-1$

$$\mathbf{H} = \begin{cases} h_i & \text{if } i = j \\ 0 & \text{otherwise} \end{cases}, \quad (2.3)$$

where  $h_n, n = 0, \dots, N-1$ , is the channel response of the  $n$ -th sub-carrier. Finally,

$$\mathbf{F} = \frac{1}{\sqrt{N}} \begin{bmatrix} 1 & 1 & 1 & \dots & 1 \\ 1 & e^{-j\frac{2\pi}{N}1 \cdot 1} & e^{-j\frac{2\pi}{N}1 \cdot 2} & \dots & e^{-j\frac{2\pi}{N}1 \cdot (N-1)} \\ 1 & e^{-j\frac{2\pi}{N}2 \cdot 1} & e^{-j\frac{2\pi}{N}2 \cdot 2} & \dots & e^{-j\frac{2\pi}{N}2 \cdot (N-1)} \\ \dots & \dots & \dots & \dots & \dots \\ 1 & e^{-j\frac{2\pi}{N}(N-1) \cdot 1} & e^{-j\frac{2\pi}{N}(N-1) \cdot 2} & \dots & e^{-j\frac{2\pi}{N}(N-1) \cdot (N-1)} \end{bmatrix} \quad (2.4)$$

is  $N \times N$  DFT matrix.

The MLD solution of the SC-FDMA setting, formulated in Eq. (2.2), is

$$\hat{\mathbf{s}}_{ML} = \underset{\mathbf{s} \in \mathcal{C}}{\operatorname{argmin}} \|\mathbf{y} - \mathbf{H}\mathbf{F}\mathbf{s}\|^2, \quad (2.5)$$

where  $\mathcal{C}$  is the space of all length- $N$  vectors whose alphabet are symbols drawn from some constellation (QAM, PSK). Although the MLD solution in Eq. (2.5) is optimal, its computation is impractical since its complexity grows exponentially fast with the SC DFT size  $N$ . There are alternative linear detection schemes for the SC-FDMA settings. In a linear detection scheme, the measurement  $\mathbf{y}$  in Eq. (2.2) is multiplied by a matrix  $\mathbf{W}$ , to produce the signal estimate  $\hat{\mathbf{s}}$ . The matrix  $\mathbf{W}$  was chosen according to the detector type and, in general, it is not an orthogonal matrix. Therefore, linear detection (and specifically FDE) is sub-optimal, especially in a distributed SC-FDMA setting where the fading channel is characterized by more frequency selectivity over the sub-carriers that are associated with the DFT block. In this case, frequency-domain equalization will distort the whiteness of the noise, thus making the inputs to the inverse DFT unequally reliable. Formally,

$$\begin{aligned} \hat{\mathbf{s}}_{ML} &\triangleq \underset{\mathbf{s} \in \mathcal{C}}{\operatorname{argmin}} \|\mathbf{y} - \mathbf{H}\mathbf{F}\mathbf{s}\|^2 = \underset{\mathbf{s} \in \mathcal{C}}{\operatorname{argmin}} [(\mathbf{y} - \mathbf{H}\mathbf{F}\mathbf{s})^T (\mathbf{y} - \mathbf{H}\mathbf{F}\mathbf{s})] \\ &\neq \underset{\mathbf{s} \in \mathcal{C}}{\operatorname{argmin}} [(\mathbf{y} - \mathbf{H}\mathbf{F}\mathbf{s})^T \mathbf{W}^T \mathbf{W} (\mathbf{y} - \mathbf{H}\mathbf{F}\mathbf{s})] = \underset{\mathbf{s} \in \mathcal{C}}{\operatorname{argmin}} \|\mathbf{W}(\mathbf{y} - \mathbf{H}\mathbf{F}\mathbf{s})\|^2 = \hat{\mathbf{s}}_{FDE-MLD}. \end{aligned}$$

## 2.1 Motivation

Evaluating the performance of ML detection is important for providing a reference point for alternative, sub-optimal, detection schemes for SC-FDMA. It is, however, typically impractical to simulate. In this work, we derive an approximation for the BER obtained when applying the MLD scheme to uncoded SC-FDMA setting in a Rayleigh fading environment.

The Rayleigh fading channel model is a standard model - see [3, 9]. According to this model, the real and the imaginary parts of each tap of the channel's impulse response are distributed independently and normally according to a Gaussian probability distribution function

$$f_x(x) = \frac{1}{\sqrt{2\pi}\sigma^2} \exp \left\{ -\frac{x^2}{2\sigma^2} \right\},$$

where  $\sigma$  is the standard deviation. It follows that a tap's amplitude is distributed according to the following probability distribution function

$$f_{|h[k]|}(a) = \frac{a}{\sigma^2} \exp \left\{ -\frac{a^2}{2\sigma^2} \right\}, a \geq 0.$$

This is called Rayleigh distribution. The frequency domain channel response can be regarded as a weighted sum of time domain taps which are complex Gaussian variables. Therefore, the frequency domain samples of the channel response are themselves complex Gaussian RV with a certain correlation. In the case of a single tap fading channel (Line of Sight), the frequency channel response samples are fully correlated forming flat fading. In this case, the delay spread is zero and the coherence bandwidth is maximal. On the other hand, in the case of infinite delay spread of the channel impulse response, the coherence bandwidth is zero. This channel model is called uncorrelated (in frequency) Rayleigh fading channel. In between these two extreme correlated channels cases, there are other correlated fading channel models including the standard ITU models. For instance, ITU Vehicular A fading channel model has delay spread of  $0.37\mu\text{Sec}$ . and coherence bandwidth of 180 sub-carriers for a carrier spacing of 15KHz while ITU Vehicular B fading channel model has delay spread of  $4\mu\text{Sec}$ . and coherence bandwidth of 17 sub-carriers.

### 3 Error-Probability Derivation

In this section we derive a bound on the error probability of the MLD receiver defined in Eq. (2.5). The underlying principles used for deriving this bound can be traced back to [7]. For simplicity, the analysis is carried out for binary phase shift keying (BPSK) modulation. It can be extended to larger constellation sizes.

In order to evaluate the error probability, assume that a symbol  $\mathbf{s} \in \text{BPSK}^N$  was transmitted. Define a cost function

$$J(\boldsymbol{\xi}) = \|\mathbf{y} - \mathbf{H}\mathbf{F}\boldsymbol{\xi}\|^2, \quad (3.1)$$

and the minimizing vector

$$\hat{\mathbf{s}} \triangleq \underset{\boldsymbol{\xi} \in \mathcal{A}}{\text{argmin}} J(\boldsymbol{\xi}), \quad (3.2)$$

where  $\mathcal{A} = \text{BPSK}^N$  is the set of all possible transmitted vectors. Since  $\hat{\mathbf{s}}$  is the minimizer of the cost function  $J(\boldsymbol{\xi})$ , which is usually identical to  $\mathbf{s}$  at high SNR, we investigate the cost function  $J(\cdot)$  for vectors that deviate from the transmitted vector  $\mathbf{s}$ . We denote this *deviation vector* by  $\mathbf{e}$ . The  $n$ -th element of  $\mathbf{e}$  is either 0, or  $-2s_n$ ,  $s_n$  being the  $n$ -th element of  $\mathbf{s}$ . Thus, for every transmitted vector  $\mathbf{s}$  there are  $2^N - 1$  possible deviation vectors  $\mathbf{e}$  (the all-zero vector is excluded). By substituting Eq. (2.2) with the argument  $\mathbf{s} + \mathbf{e}$  into Eq.



(3.1) we get

$$\begin{aligned}
J(\mathbf{s} + \mathbf{e}) &= \|\mathbf{y} - \mathbf{H}\mathbf{F}(\mathbf{s} + \mathbf{e})\|^2 \\
&= \|\mathbf{H}\mathbf{F}\mathbf{s} + \rho\mathbf{n} - \mathbf{H}\mathbf{F}(\mathbf{s} + \mathbf{e})\|^2 \\
&= \|\rho\mathbf{n} - \mathbf{H}\mathbf{F}\mathbf{e}\|^2 \\
&= \|\mathbf{H}\mathbf{F}\mathbf{e}\|^2 + \|\rho\mathbf{n}\|^2 - 2\rho\Re\{(\mathbf{H}\mathbf{F}\mathbf{e})^*\mathbf{n}\},
\end{aligned} \tag{3.3}$$

while the cost function of the transmitted vector  $\mathbf{s}$  is

$$J(\mathbf{s}) = \|\mathbf{y} - \mathbf{H}\mathbf{F}\mathbf{s}\|^2 = \|\rho\mathbf{n}\|^2. \tag{3.4}$$

By subtracting Eq. (3.4) from Eq. (3.3) we get the cost increment due to the deviation from  $\mathbf{s}$  to be

$$\Delta J(\mathbf{e}) \triangleq J(\mathbf{s} + \mathbf{e}) - J(\mathbf{s}) = \|\mathbf{H}\mathbf{F}\mathbf{e}\|^2 - 2\rho\Re\{(\mathbf{H}\mathbf{F}\mathbf{e})^*\mathbf{n}\}. \tag{3.5}$$

For given  $\mathbf{H}$  and  $\mathbf{e}$ ,  $\Delta J(\mathbf{e})$  is a Gaussian random variable (RV) with expectation  $E\{\Delta J(\mathbf{e})\} = \|\mathbf{H}\mathbf{F}\mathbf{e}\|^2$  and variance  $\text{Var}\{\Delta J(\mathbf{e})\} = 2\rho^2\|\mathbf{H}\mathbf{F}\mathbf{e}\|^2$ . Thus, the probability that the cost of  $\mathbf{s} + \mathbf{e}$  is smaller than  $\mathbf{s}$  is

$$\begin{aligned}
\Pr\{\mathbf{e}|\mathbf{H}\} &\triangleq \Pr\{\Delta J(\mathbf{e}) < 0|\mathbf{H}\} = \\
&= \frac{1}{\sqrt{4\pi\rho^2\|\mathbf{H}\mathbf{F}\mathbf{e}\|^2}} \int_{-\infty}^0 \exp\left\{-\frac{(x - \|\mathbf{H}\mathbf{F}\mathbf{e}\|^2)^2}{2 \cdot 2\rho^2\|\mathbf{H}\mathbf{F}\mathbf{e}\|^2}\right\} dx \\
&= \frac{1}{\sqrt{4\pi\rho^2\|\mathbf{H}\mathbf{F}\mathbf{e}\|^2}} \int_0^{\infty} \exp\left\{-\frac{(x + \|\mathbf{H}\mathbf{F}\mathbf{e}\|^2)^2}{2 \cdot 2\rho^2\|\mathbf{H}\mathbf{F}\mathbf{e}\|^2}\right\} dx.
\end{aligned} \tag{3.6}$$

Equation (3.6) can be reformulated simply as

$$\Pr\{\mathbf{e}|\mathbf{H}\} = Q\left(\frac{\|\mathbf{H}\mathbf{F}\mathbf{e}\|}{\sqrt{2}\rho}\right), \tag{3.7}$$

where  $Q(x) = \frac{1}{\sqrt{2\pi}} \int_x^{\infty} e^{-\frac{y^2}{2}} dy$ . Denote the number of errors in the deviation vector  $\mathbf{e}$  of size  $N \times 1$  by  $n_e$  ( $0 \leq n_e \leq N$ ). Therefore, the exact BER conditioned on  $\mathbf{H}$  is

$$P_b = E\left\{\frac{n_e}{N}\right\} = \sum_{n_e=1}^N \frac{n_e}{N} \cdot \Pr\{n_e|\mathbf{H}\}, \tag{3.8}$$

where  $\Pr\{n_e|\mathbf{H}\} = \Pr\{\bigcup\{\mathbf{e} : \text{number of errors is } n_e\}|\mathbf{H}\}$  is the probability that the deviation vector  $\mathbf{e}$  contains exactly  $n_e$  non-zero elements. By using a union bound for  $\Pr\{n_e|\mathbf{H}\}$ , we get that  $\Pr\{n_e|\mathbf{H}\} \leq \sum_{\mathbf{e}:n_e} \Pr\{\mathbf{e}|\mathbf{H}\}$ . Therefore, the upper bound on the bit error probability is

$$P_b(\mathbf{H}) \leq \sum_{n_e=1}^N \frac{n_e}{N} \cdot \sum_{\mathbf{e}:n_e} \Pr\{\mathbf{e}|\mathbf{H}\} = \sum_{\mathbf{e}} \frac{n_e}{N} \cdot \Pr\{\mathbf{e}|\mathbf{H}\}. \tag{3.9}$$

Substituting Eq. (3.7) into Eq. (3.9) we get

$$P_b(\mathbf{H}) \leq \sum_{\mathbf{e}} \frac{n_e}{N} \cdot Q\left(\frac{\|\mathbf{H}\mathbf{F}\mathbf{e}\|}{\sqrt{2\rho}}\right). \quad (3.10)$$

On the other hand, by identifying the most probable error vector  $\mathbf{e}_o$ , we can derive the following lower bound from Eqs. (3.7) and (3.8)

$$P_b(\mathbf{H}) \geq \frac{n_e(\mathbf{e}_o)}{N} \cdot Q\left(\frac{\|\mathbf{H}\mathbf{F}\mathbf{e}_o\|}{\sqrt{2\rho}}\right), \quad (3.11)$$

where  $\mathbf{e}_o = \underset{\mathbf{e} \in \mathcal{E}}{\operatorname{argmin}}\{\|\mathbf{H}\mathbf{F}\mathbf{e}\|\}$  and  $\mathcal{E}$  is the set of all possible deviation vectors. Note that the bounds (3.10) and (3.11) are difficult to calculate due to the fact that there are  $2^N - 1$  different deviation vectors. Therefore, these bounds can be used only for cases where the DFT size is sufficiently small.

The performance of the classical flat fading OFDM setting can be derived from Eq. (3.7) assuming the matrices  $\mathbf{F}$  and  $\mathbf{H}$  are of sizes  $1 \times 1$ . In this case,  $\mathbf{F} = 1$  and  $\mathbf{H}$  is a scalar denoted by  $h$ ; hence, the error probability is

$$\Pr\{e|h\} = Q\left(\frac{\|h \cdot 1 \cdot e\|}{\sqrt{2\rho}}\right) = Q\left(\sqrt{2 \cdot \text{SNR}}\right), \quad (3.12)$$

where  $\text{SNR} \triangleq \frac{1}{\rho^2}$ . Note that Eq. (3.12) constitutes the well known result for the flat fading OFDM case.

## 4 Closed-Form Bounds for the Error Probability

In this section, we derive the approximated lower-bounds for the BER performance (3.11). Assume that the channel response matrix  $\mathbf{H}$  is a diagonal matrix of Rayleigh distribution with a covariance matrix  $\mathbf{C}$ . Then, we integrate Eq. (3.7) to get the average error probability

$$\Pr\{\mathbf{e}\} = \int \Pr\{\mathbf{e}|\mathbf{H}\} \Pr\{\mathbf{H}\} d\mathbf{H} = \int Q\left(\frac{\|\mathbf{H}\mathbf{F}\mathbf{e}\|}{\sqrt{2\rho}}\right) \frac{1}{\pi^N \det(\mathbf{C})} \exp\{-\mathbf{h}^* \mathbf{C}^{-1} \mathbf{h}\} d\mathbf{h}, \quad (4.1)$$

where  $\mathbf{h}$  denotes the diagonal of the channel matrix  $\mathbf{H}$  and  $\det(\mathbf{C}) \neq 0$ . Using the upper bound for the Q-function  $Q(x) \leq \frac{1}{2} \exp\left(-\frac{x^2}{2}\right)$ , we get

$$\Pr\{\mathbf{e}\} \leq \frac{1}{2} \int \exp\left\{-\frac{\|\mathbf{H}\mathbf{F}\mathbf{e}\|^2}{4\rho^2}\right\} \frac{1}{\pi^N \det(\mathbf{C})} \exp\{-\mathbf{h}^* \mathbf{C}^{-1} \mathbf{h}\} d\mathbf{h}. \quad (4.2)$$

Since the matrix  $\mathbf{H}$  is diagonal, the expression  $\|\mathbf{H}\mathbf{F}\mathbf{e}\|^2$  can be rewritten as

$$\begin{aligned}\|\mathbf{H}\mathbf{F}\mathbf{e}\|^2 &= (\mathbf{F}\mathbf{e})^* \text{diagm}\{\mathbf{h}\}^* \text{diagm}\{\mathbf{h}\} (\mathbf{F}\mathbf{e}) \\ &= \mathbf{h}^* \text{diagm}\{\mathbf{F}\mathbf{e}\}^* \text{diagm}\{\mathbf{F}\mathbf{e}\} \mathbf{h} \\ &= \mathbf{h}^* \mathbf{M} \mathbf{h},\end{aligned}\tag{4.3}$$

where  $\mathbf{f}_1, \dots, \mathbf{f}_N$  are the rows of the DFT matrix  $\mathbf{F}$  (2.4),  $\text{diagm}\{\mathbf{x}\}$  forms a square matrix whose diagonal is  $\mathbf{x}$  and off-diagonal elements are zeros and  $\mathbf{M} \triangleq \text{diagm}\{|\mathbf{f}_1\mathbf{e}|^2, \dots, |\mathbf{f}_N\mathbf{e}|^2\}$ .

Substituting Eq. (4.3) into Eq. (4.2) we get

$$\begin{aligned}\Pr\{\mathbf{e}\} &\leq \frac{1}{2} \int \exp\left\{-\mathbf{h}^* \frac{\mathbf{M}}{4\rho^2} \mathbf{h}\right\} \frac{1}{\pi^N \det(\mathbf{C})} \exp\{-\mathbf{h}^* \mathbf{C}^{-1} \mathbf{h}\} d\mathbf{h} \\ &= \frac{1}{2\pi^N \det(\mathbf{C})} \int \exp\left\{-\mathbf{h}^* \left(\frac{\mathbf{M}}{4\rho^2} + \mathbf{C}^{-1}\right) \mathbf{h}\right\} d\mathbf{h}.\end{aligned}\tag{4.4}$$

Since the PDF of a complex Gaussian vector  $\mathbf{x}$  of length  $L$  with autocovariance  $\mathbf{V}$  takes the form  $\frac{1}{\pi^L \det(\mathbf{V})} \exp\{\mathbf{x}^* \mathbf{V}^{-1} \mathbf{x}\}$  and its integral equals 1, then we can rewrite Eq. (4.4) as

$$\begin{aligned}\Pr\{\mathbf{e}\} &\leq \frac{1}{2\det(\mathbf{C})} \left[ \det\left(\frac{\mathbf{M}}{4\rho^2} + \mathbf{C}^{-1}\right) \right]^{-1} \\ &= \frac{1}{2} \left[ \det\left(\frac{\mathbf{M}}{4\rho^2} \mathbf{C} + \mathbf{I}\right) \right]^{-1}.\end{aligned}\tag{4.5}$$

The error probability bound in Eq. (4.5) depends on the deviation vector  $\mathbf{e}$ .

Denote by  $b_n$  the specific bit number  $n$  in the vector  $\mathbf{s}$ . The probability of error in bit  $b_n$  satisfies

$$P_b(n) = \Pr\{\mathcal{E}_n\} \geq \max_{\mathbf{e} \in \mathcal{E}_n} \Pr\{\mathbf{e}\},\tag{4.6}$$

where  $\mathcal{E}_n$  is the subset of  $\mathcal{E}$  in which all the deviation vectors contain an error in the  $n$ -th position.

There are cases for which we can calculate the lower bound defined in Eq. (4.6). Next, we derive explicit closed form expressions for some of these cases.

## 4.1 Uncorrelated Fading Channel Case

We examine the particular case of an uncorrelated Rayleigh channel. In this case,  $\mathbf{C} = \sigma^2 \mathbf{I}$  and Eq. (4.5) becomes

$$\begin{aligned}
\Pr\{\mathbf{e}\} &\leq \frac{1}{2} \left[ \det \left( \frac{\sigma^2}{4\rho^2} \mathbf{M} + \mathbf{I} \right) \right]^{-1} \\
&= \frac{1}{2} \left[ \det \left( \frac{\sigma^2}{4\rho^2} \text{diagm}\{|\mathbf{f}_1 \mathbf{e}|^2, \dots, |\mathbf{f}_N \mathbf{e}|^2\} + \mathbf{I} \right) \right]^{-1} \\
&= \left( 2 \left( \frac{\sigma^2}{4\rho^2} |\mathbf{f}_1 \mathbf{e}|^2 + 1 \right) \left( \frac{\sigma^2}{4\rho^2} |\mathbf{f}_2 \mathbf{e}|^2 + 1 \right) \cdots \left( \frac{\sigma^2}{4\rho^2} |\mathbf{f}_N \mathbf{e}|^2 + 1 \right) \right)^{-1} \\
&= \frac{1}{2} \prod_{n=1}^N \left( \frac{1}{4} |\mathbf{f}_n \mathbf{e}|^2 \text{SNR} + 1 \right)^{-1}.
\end{aligned} \tag{4.7}$$

Based on the Eq. (4.7), we derive the bounds for  $P_b$  in high and low SNR regimes.

### 4.1.1 High SNR Regime

We present a lemma that will be useful for the derivation of our main theorem. Let us first define the following condition:

**Condition 1.** A vector  $\mathbf{e}$  is said to satisfy *Condition 1*, if  $\text{DFT}(\mathbf{e}) = \mathbf{F}\mathbf{e}$  has a single non-zero element.

**Lemma 4.1.** *For any DFT of size  $N$  (even) there are exactly 4 possible transmitted BPSK vectors such that there is a valid deviation vector satisfying Condition 1.*

*Proof.* The rows of the DFT matrix ( $\mathbf{f}_k = e^{-j\theta n}, \theta = \frac{2\pi}{N}k, n = 0, \dots, N-1$ ) are the basis for the  $N$ -th length vector space. The deviation vector  $\mathbf{e}$  can be represented as  $\mathbf{e} = \sum_{k=0}^{N-1} (\mathbf{f}_k \mathbf{e}^*) \mathbf{f}_k$ . Therefore, the deviation vector  $\mathbf{e}$  satisfies Condition 1 and it can be any of the DFT matrix rows that are multiplied by 2, or -2. The fact that the deviation vector is real, implies that only two rows of  $F$  are relevant where  $\theta = 0$  and  $\theta = \pi$ . This means that only 4 deviation vectors satisfy the condition in the Lemma. They are  $\pm[2, 2, 2, 2, \dots, 2, 2]$ . They correspond to  $\theta = 0$  and  $\pm[2, -2, 2, -2, \dots, 2, -2]$  correspond to  $\theta = \pi$ . The corresponding 4 (out of  $2^N$ ) transmitted vectors are  $\mp[1, 1, 1, 1, \dots, 1, 1]$  and  $\mp[1, -1, 1, -1, \dots, 1, -1]$ .  $\square$

**Theorem 4.2.**

$$\lim_{\text{SNR} \rightarrow \infty} P_b^{(MLD)} = \frac{1}{N 2^N \text{SNR}}. \tag{4.8}$$

*Proof.* For high SNR the deviation vector with the smallest diversity order (DO) dominates the error probability [2]. The DO is defined in [2] as

$$\text{DO} \triangleq - \lim_{\text{SNR} \rightarrow \infty} \frac{\log_e \Pr \{\text{error}\}}{\log_e \text{SNR}}. \quad (4.9)$$

The DO, which is associated with  $\Pr \{\mathbf{e}\}$ , is computed by using Eqs. (4.9) and (4.7)

$$\begin{aligned} \text{DO}\{\Pr \{\mathbf{e}\}\} &= - \lim_{\text{SNR} \rightarrow \infty} \frac{\log_e \Pr \{\mathbf{e}\}}{\log_e \text{SNR}} \\ &\geq \lim_{\text{SNR} \rightarrow \infty} \frac{\log_e 2 \prod_{n=1}^N \left( \frac{1}{4} |\mathbf{f}_n \mathbf{e}|^2 \text{SNR} + 1 \right)}{\log_e \text{SNR}} \\ &\geq \lim_{\text{SNR} \rightarrow \infty} \left( \frac{\log_e 2 \prod_{n: \mathbf{f}_n \mathbf{e} \neq 0} \frac{1}{4} |\mathbf{f}_n \mathbf{e}|^2}{\log_e \text{SNR}} \right) \\ &+ \lim_{\text{SNR} \rightarrow \infty} \left( \frac{\log_e \text{SNR}^K}{\log_e \text{SNR}} \right) \\ &= 0 + K = K, \end{aligned} \quad (4.10)$$

where  $K$  is the number of non-zero elements in  $\mathbf{F}\mathbf{e}$ . Therefore, from Eq. (4.10) we conclude that the DO, which is associated with  $\Pr \{\mathbf{e}\}$ , is greater or equal to the number of non-zero elements in  $\mathbf{F}\mathbf{e}$ .

Specifically, a deviation vector  $\mathbf{e}_x$ , which satisfies Condition 1, results with the following error probability

$$\begin{aligned} \Pr \{\mathbf{e}_x\} &= \int \Pr \{\mathbf{e}_x | \mathbf{H}\} \Pr \{\mathbf{H}\} d\mathbf{H} \\ &= \int Q \left( \frac{\|\mathbf{H}\mathbf{F}\mathbf{e}_x\|}{\sqrt{2\rho}} \right) P(\mathbf{H}) d\mathbf{H} \\ &= \int Q \left( \sqrt{2N \text{SNR}} y \right) 2y \exp(-y^2) dy, \end{aligned} \quad (4.11)$$

where  $y = |h|$  is a Rayleigh distributed scalar. By substituting Eq. (A.1) with the argument  $2N \text{SNR}$  into (4.11) we get

$$\Pr \{\mathbf{e}_x\} = \frac{1}{4N \text{SNR}}. \quad (4.12)$$

The DO from Eq. (4.12) is

$$\text{DO}\{\Pr \{\mathbf{e}_x\}\} = \lim_{\text{SNR} \rightarrow \infty} \frac{\log_e 4N \text{SNR}}{\log_e \text{SNR}} = 1. \quad (4.13)$$

From (4.13) and (4.10) it follows that  $\mathbf{e}_x$ , which satisfies Condition 1, produces the error probability with the smallest DO. Therefore, it dominates the error probability in the high

SNR regime. However, in order to get the explicit lower bound on the bit error probability, we have to take into account that not all the possible deviation vectors are valid for a given transmitted vector  $\mathbf{s}$ . For example, all the elements of the deviation vector  $\mathbf{e}$  may be equal to 2 with a non zero probability, only if all the elements of the transmitted vector  $\mathbf{s}$  are equal to -1. Lemma (4.1) shows that there are exactly 4 possible BPSK vectors of an even length  $N$  that satisfy Condition 1. In other words, the probability for transmitted vector with DO=1 is  $\frac{4}{2^N}$ . Multiplying Eq. (4.12) by this factor, we get that the MLD bit-error probability, for SC-FDMA in an uncorrelated Rayleigh fading channel, is lower bounded by

$$P_b^{(MLD)}(\text{high SNR}) \geq \frac{4}{2^N} \frac{1}{4N \text{SNR}} = \frac{1}{N2^N \text{SNR}}.$$

□

One can see from Eq. (4.8) that the array gain grows (and the error probability curve shifts to the left) as the DFT size  $N$  increases. This is true in the setting being used in this work, i.e. uncoded transmission over an uncorrelated fading channel. In a practical system such as OFDMA, the channel diversity will be utilized by means of coding, interleaving and allocation techniques. Therefore, the performance difference between OFDMA and SC-FDMA with different DFT sizes is expected to be small.

#### 4.1.2 Low SNR Regime

In order to identify the error vector, which has the highest probability, Eq. (4.7) was developed for low SNR regime as follows

$$\begin{aligned} \Pr\{\mathbf{e}\} &\leq \frac{1}{2} \prod_{n=1}^N \left( \frac{1}{4} |\mathbf{f}_n \mathbf{e}|^2 \text{SNR} + 1 \right)^{-1} = \frac{1}{2 \prod_{n=1}^N \left( \frac{1}{4} |\mathbf{f}_n \mathbf{e}|^2 \text{SNR} + 1 \right)} \\ &\approx \frac{1}{2 \left( 1 + \sum_{n=1}^N \frac{1}{4} |\mathbf{f}_n \mathbf{e}|^2 \text{SNR} \right)} = \frac{1}{2 \left( 1 + \frac{1}{4} \text{SNR} \sum_{n=1}^N |\mathbf{f}_n \mathbf{e}|^2 \right)} \\ &= \frac{1}{2 \left( 1 + \frac{1}{4} \text{SNR} \|\mathbf{e}\|^2 \right)}. \end{aligned} \quad (4.14)$$

The  $\Pr\{\mathbf{e}\}$  is upper bounded by the expression (4.14), which is maximal for the error vectors of smallest norm. Therefore, we assume that the error vectors with only one non zero

element (i.e. smallest norm) are the dominant error vectors in the low SNR regime. Based on the following Q-function approximation  $Q(x) \approx \frac{1}{12} \exp\left\{-\frac{x^2}{2}\right\} + \frac{1}{4} \exp\left\{-\frac{4}{3}\frac{x^2}{2}\right\}$  ([7]), an expression similar to (4.5), as derived from (4.1), is given by

$$\begin{aligned} \Pr\{\mathbf{e}\} &= \frac{1}{12} \left[ \det \left( \frac{\text{diagm}\{|\mathbf{f}_1 \mathbf{e}|^2, \dots, |\mathbf{f}_N \mathbf{e}|^2\}}{4\rho^2} \mathbf{C} + \mathbf{I} \right) \right]^{-1} \\ &+ \frac{1}{4} \left[ \det \left( \frac{4}{3} \frac{\text{diagm}\{|\mathbf{f}_1 \mathbf{e}|^2, \dots, |\mathbf{f}_N \mathbf{e}|^2\}}{4\rho^2} \mathbf{C} + \mathbf{I} \right) \right]^{-1}. \end{aligned} \quad (4.15)$$

Substituting  $\mathbf{e} = [2, 0, \dots, 0]$ , and  $\mathbf{f}_1, \dots, \mathbf{f}_N$  into (4.15), we get an approximated lower bound for the BER in the low SNR regime

$$P_b^{(MLD)}(\text{low SNR}) \geq \frac{1}{12} \left( 1 + \frac{1}{N} \text{SNR} \right)^{-N} + \frac{1}{4} \left( 1 + \frac{4}{3N} \text{SNR} \right)^{-N}. \quad (4.16)$$

## 4.2 Correlated Fading Channel Case

In a correlated Rayleigh channel with the correlation matrix  $\mathbf{C}$ , the deviation vector with the smallest DO is the same as in the uncorrelated case (4.8). This is true because substituting a deviation vector, which satisfies Condition 1, yields an expression which is linear in the SNR and therefore DO=1. For example, by substituting  $\mathbf{e} = [2, 2, \dots, 2]$  into the determinant in Eq. (4.5), we get

$$\begin{aligned} &\det \left( \frac{\text{diagm}\{|\mathbf{f}_1 \mathbf{e}|^2, \dots, |\mathbf{f}_N \mathbf{e}|^2\}}{4\rho^2} \mathbf{C} + \mathbf{I} \right) = \\ &= \det \left( \begin{bmatrix} N \cdot \text{SNR} & 0 & \dots & 0 \\ 0 & 0 & \dots & 0 \\ \dots & \dots & \dots & \dots \\ 0 & 0 & \dots & 0 \end{bmatrix} + \begin{bmatrix} 1 & c_{1,2} & \dots & c_{1,N} \\ c_{2,1} & 1 & \dots & c_{2,N} \\ \dots & \dots & \dots & \dots \\ c_{N,1} & c_{N,2} & \dots & 1 \end{bmatrix} + \begin{bmatrix} 1 & 0 & \dots & 0 \\ 0 & 1 & \dots & 0 \\ \dots & \dots & \dots & \dots \\ 0 & 0 & \dots & 1 \end{bmatrix} \right) = \\ &= \det \left( \begin{bmatrix} N \cdot \text{SNR} + 1 & c_{1,2} N \cdot \text{SNR} & \dots & c_{1,N} N \cdot \text{SNR} \\ 0 & 1 & \dots & 0 \\ \dots & \dots & \dots & \dots \\ 0 & 0 & \dots & 1 \end{bmatrix} \right) = \\ &= N \cdot \text{SNR} + 1. \end{aligned} \quad (4.17)$$

For any other non-zero deviation vector, which does not satisfy Condition 1, (4.17) will be a polynomial of degree at least 2 of the SNR. Consequently, the corresponding BER will be affected by DO of at least 2. Therefore, when  $\det(\mathbf{C}) \neq 0$ , the asymptotical lower bound of the BER for a correlated Rayleigh channel is the same as the one for the uncorrelated Rayleigh channel (4.8).

As a sanity check, let us examine a flat fading Rayleigh channel as a particular case for which  $\det(\mathbf{C}) = 0$ . In this case, Eq. (4.1) no longer holds since the distribution function contains division by  $\det(\mathbf{C})$ . Instead, we can rewrite Eq. (3.7) for a flat fading case:  $\mathbf{H} = h \cdot \mathbf{I}$ , where  $h$  is a complex scalar with a Gaussian distribution, and hence

$$\Pr\{\mathbf{e}|\mathbf{H}\} = Q\left(\frac{\|\mathbf{H}\mathbf{F}\mathbf{e}\|}{\sqrt{2\rho}}\right) = Q\left(\frac{|h| \cdot \|\mathbf{F}\mathbf{e}\|}{\sqrt{2\rho}}\right) = Q\left(\frac{|h| \cdot \|\mathbf{e}\|}{\sqrt{2\rho}}\right). \quad (4.18)$$

Therefore,

$$P_b \approx \Pr\{\mathbf{e} : 1 \text{ non zero element}|\mathbf{H}\} = Q\left(\sqrt{2 \cdot \text{SNR}}\right), \quad (4.19)$$

which is identical to the OFDM BER formula (Eq. (3.12)). Since the performance of SC-FDMA in a Rayleigh channel can only be better than those obtained in a flat fading channel, we use the OFDM BER curve for upper bounding the BER performance of SC-FDMA.

It follows from the above derivation and from Fig. 5.1 that the BER curves for MLD of SC-FDMA over Rayleigh channel are upper bounded by the OFDM BER performance (4.19) and lower bounded by (4.8).

## 5 Simulation Results

In order to verify the approximations (4.8) and (4.16), we simulated MLD for SC-FDMA with DFT sizes of 2,4,8 in an uncorrelated Rayleigh fading environment. The simulation results with the corresponding bounds are presented in Fig. 5.1. The Matlab simulation took approximately 24 hours on a standard PC equipped with 1.8GHz processor and 2GB RAM. In contrast to the exact lower bound on the MLD BER (4.6), the presented bounds are easy to calculate for any DFT size. Evidently, the simulated BER curves converge to the lower bound in the high SNR regime.

The dependance of the BER on the channel correlation is demonstrated in Fig. 5.2. The top curve, which is used here as a reference, presents the BER performance for OFDM. All



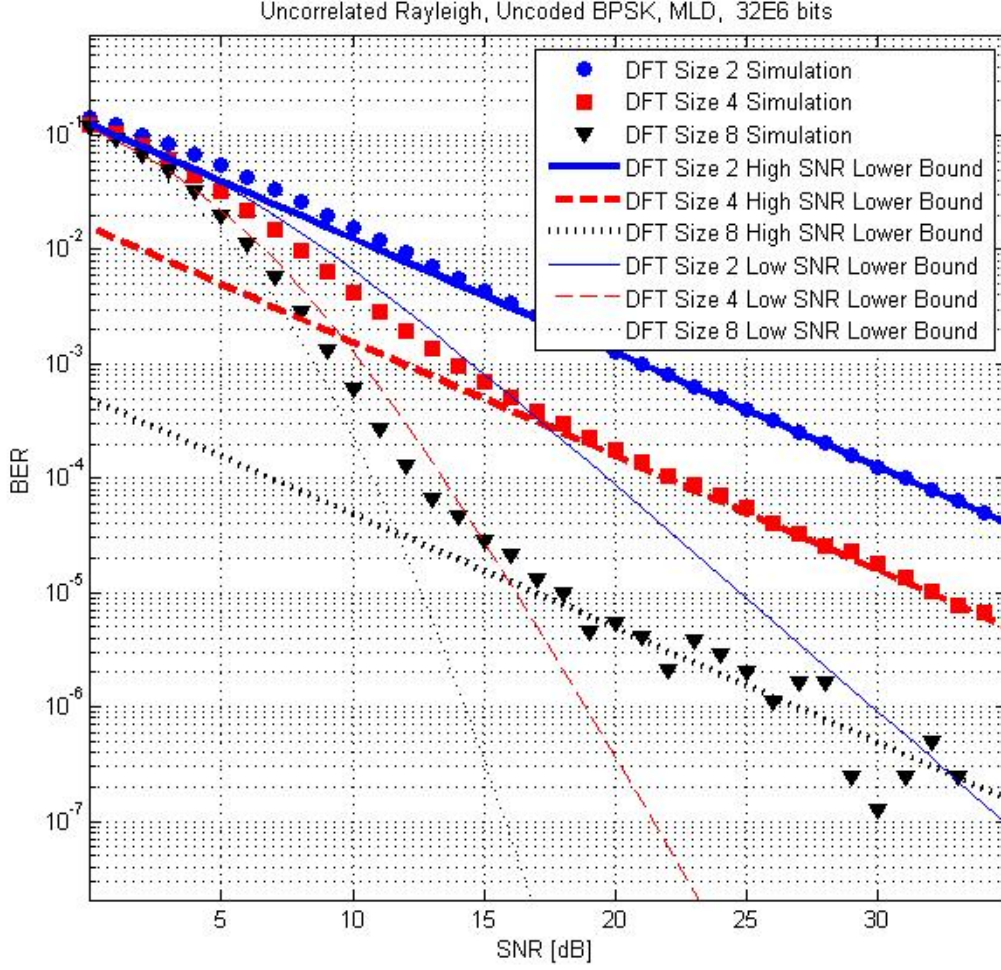


Figure 5.1: BER of MLD applied to SC-FDMA (DFT sizes 2,4,8) over an uncorrelated Rayleigh channel using uncoded BPSK modulation.

the other curves correspond to the BER performance of SC-FDMA (DFT of size 4) MLD over a Rayleigh fading channel with correlation function  $r[n] = \exp\{-n/K\}$ , where  $n$  is the sub-carrier index and  $K$  is the fading-channel correlation parameter. We studied the correlation function for the following values of the parameter  $K$ : 3,6,30,100, 1000. The MatLab simulation took approximately 4 hours on a standard PC equipped with 1.8GHz processor and 2GB RAM. From Fig. 5.2, we conclude that the BER curve for the Rayleigh fading channel, with correlation function defined above, is upper bounded by the OFDM BER curve (4.19) and lower bounded by the lower bound in the high SNR regime (4.8).

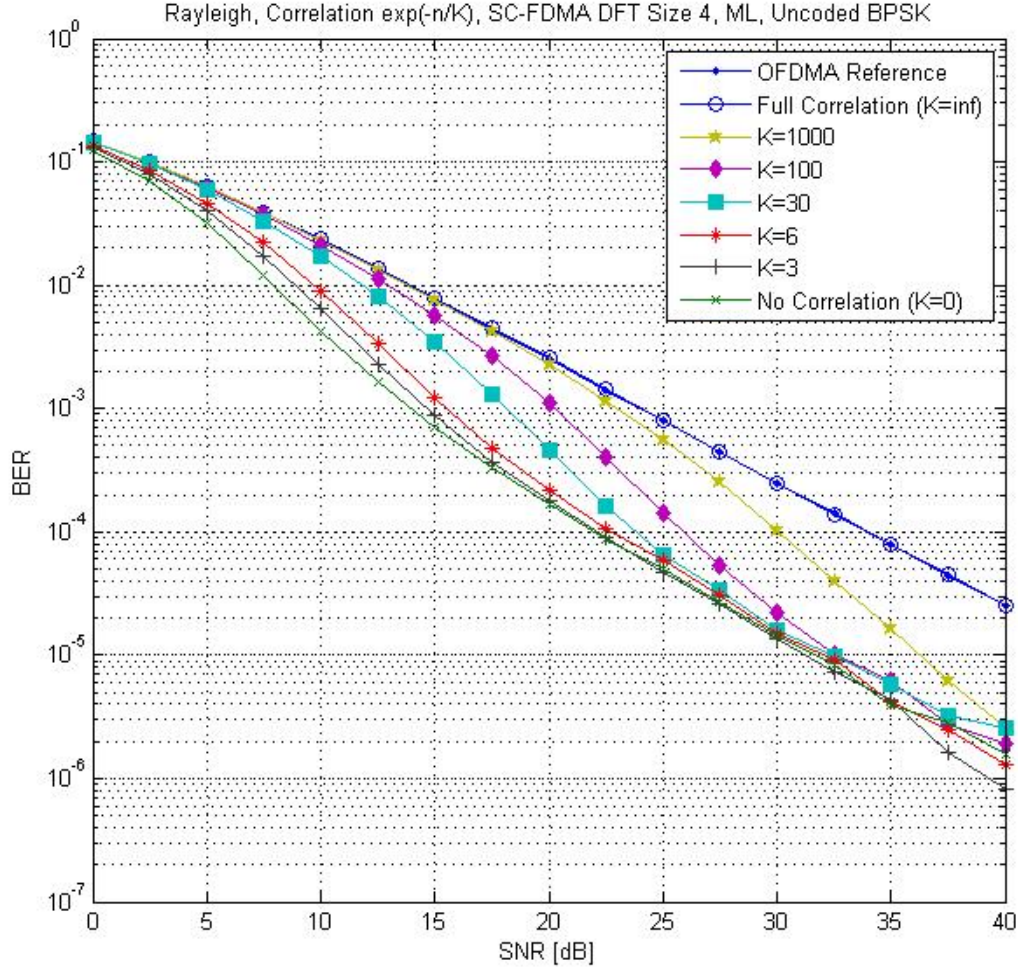


Figure 5.2: BER of MLD applied to SC-FDMA (DFT size 4) over a correlated Rayleigh channel using uncoded BPSK modulation. The correlation function is  $r[n] = \exp\{-\frac{n}{K}\}$ , where  $n$  is the sub-carrier index and  $K$  is a constant.

Moreover, all the curves except the one that corresponds to fully correlated fading channel, converge to the lower bound in the high SNR regime.

## 6 Conclusions

In this work, we present lower bounds for bit error rates of MLD, which is applied to SC-FDMA setting for a particular case when the transmission is uncoded and the fading channel

obeys the Rayleigh channel model. First, we derived upper (Eq. 3.10) and lower (Eq. 3.11) bounds for the BER performance. The bounds are formulated as a function of the fading channel realization. They are computationally expensive and, therefore, difficult to employ in practice.

Next, we derived simpler approximated lower bounds for the BER performance in an uncorrelated Rayleigh-fading channel in high (Eq. 4.8) and low (Eq. 4.16) SNR regimes. The derivations are based on identifying the Euclidean error sequences that dominate the receiver BER performance. These derivations were validated by simulation.

We demonstrated that in the fully correlated (flat fading) channel case, the derived lower bound in the high SNR regime (Eq. 4.8) coincides with the BER performance of an OFDM scheme. Furthermore, we showed that the BER of a correlated Rayleigh channel, with a covariance matrix  $\mathbf{C}$  that satisfies  $\det(\mathbf{C}) \neq 0$ , converges (asymptotically with the SNR) to the lower bound for the BER performance of the uncorrelated Rayleigh channel (Eq. 4.8).

For a correlated Rayleigh channel with a covariance matrix whose elements satisfy  $c[m, n] = e^{-\frac{|m-n|}{K}}$ , we found that the BER performance curves of SC-FDMA are located between the BER performance of OFDM in the flat fading channel (4.19) and the lower bound for the BER of SC-FDMA in an uncorrelated Rayleigh (4.8). These two can be regarded as upper and lower bounds, respectively, for the BER performance in a Rayleigh channel.

## References

- [1] “3GPP TS 36.213 E-UTRA Physical Layer Procedures.”
- [2] A. Paulraj, R. Nabar and D. Gore, *Introduction to Space Time Wireless Communications*. Cambridge University Press, 2003.
- [3] D. Tse and P. Viswanath, *Fundamental of Wireless Communication*. Cambridge University Press, 2005.
- [4] H. G. Myung, J. Lim and D. J. Goodman, “Peak-To-Average Power Ratio of Single Carrier FDMA Signals with Pulse Shaping,” *The 17th Annual IEEE International Symposium on Personal, Indoor and Mobile Radio Communications*, 2006.

- [5] H. G. Myung, J. Lim, and D. J. Goodman, “Single Carrier FDMA for Uplink Wireless Transmission,” *IEEE Vehicular Technology Magazine*, vol. 1, no. 3, pp. 30–38, 2006.
- [6] H. Wang, X. You, B. Jiang and X. Gao, “Performance Analysis of Frequency Domain Equalization in SC-FDMA Systems,” *IEEE International Communications Conference*, pp. 4342–4347, 2008.
- [7] M. Chiani and D. Dardan, “Improved Exponential Bounds and Approximation for the Q-function with Application to Average Error Probability Computation,” *Global Telecommunications Conference IEEE*, vol. 2, pp. 1399–1402, 2002.
- [8] M.D. Nisar, H. Nottensteiner, T. Hindelang, “On Performance Limits of DFT Spread OFDM Systems,” *Mobile and Wireless Communications Summit*, pp. 1–4, 2007.
- [9] S. Haykin and M. Moher, *Modern Wireless Communication*. Prentice-Hall, Inc., 2004.

## A Q-Function Integration w.r.t. Rayleigh Distribution

A simple solution for the integral of Q-function w.r.t the Rayleigh distribution is presented in this appendix.

**Lemma A.1.**

$$\int_0^\infty Q(ay) P_{\text{Rayleigh}}(y) dy = \frac{1}{2} \left( 1 - \frac{1}{\sqrt{1 + \frac{2}{a^2}}} \right) \approx \frac{1}{2a^2}.$$

*Proof.*

$$\begin{aligned} \Pr \{\text{error}\} &= \int_0^\infty Q(ay) P_{\text{Rayleigh}}(y) dy \\ &= \int_{y=0}^\infty \int_{x=ay}^\infty \frac{1}{\sqrt{2\pi}} \exp(-x^2/2) 2y \exp(-y^2) dx dy. \end{aligned} \tag{A.1}$$

By substituting  $z \triangleq \frac{x}{\sqrt{2}}$  we obtain

$$\Pr \{\text{error}\} = \frac{2}{\sqrt{\pi}} \int_{y=0}^\infty \int_{z=ay/\sqrt{2}}^\infty y \exp(-(z^2 + y^2)) dy dz. \tag{A.2}$$

We transform Eq. (A.2) from Cartesian coordinates  $\{z, y\}$  to polar coordinates  $\{r, \theta\}$  to solve this integral. Using the transformation identities  $r \sin \theta = y$ ,  $dy dz = r dr d\theta$  and defining  $\theta_o \triangleq \arctan(a/\sqrt{2})$ , we get

$$\begin{aligned} \Pr \{\text{error}\} &= \frac{2}{\sqrt{\pi}} \int_{\theta=0}^{\theta_o} \int_{r=0}^{\infty} r \sin \theta \exp(-r^2) r dr d\theta \\ &= \frac{2}{\sqrt{\pi}} \int_{\theta=0}^{\theta_o} \sin \theta d\theta \int_{r=0}^{\infty} r^2 \exp(-r^2) dr. \end{aligned} \quad (\text{A.3})$$

Substituting the standard integral  $\int_{r=0}^{\infty} r^2 \exp(-r^2) dr = \frac{\sqrt{\pi}}{4}$  into (A.3) yields

$$\Pr \{\text{error}\} = \frac{1}{2} \int_{\theta=0}^{\arctan(a/\sqrt{2})} \sin \theta d\theta = \frac{1}{2} \left( 1 - \frac{1}{\sqrt{1 + \frac{2}{a^2}}} \right). \quad (\text{A.4})$$

For high SNR, i.e  $a \rightarrow \infty$ , Equation (A.4) can be approximated by  $\sqrt{1+x} \approx 1 + x/2$ , to be

$$\Pr \{\text{error}\} \approx \frac{1}{2} \left( 1 - \frac{1}{1 + \frac{1}{a^2}} \right) \approx \frac{1}{2a^2}, \quad (\text{A.5})$$

□